ICESat observations of Arctic sea ice: A first look

Ron Kwok
Jet Propulsion Laboratory, California Institute of Technology, Pasadena, California, USA

H. Jay Zwally and Donghui Yi
Goddard Space Flight Center, Greenbelt, Maryland, USA

Received 20 April 2004; revised 22 June 2004; accepted 7 July 2004; published 18 August 2004.

[1] Analysis of near-coincident ICESat and RADARSAT imagery shows that the retrieved elevations from the laser altimeter are sensitive to new openings (containing thin ice or open water) in the sea ice cover as well as to surface relief of old and first-year ice. The precision of the elevation estimates, measured over relatively flat sea ice, is ~2 cm. Using the thickness of thin-ice in recent openings to estimate sea level references, we obtain the sea-ice freeboard along the altimeter tracks. This step is necessitated by the large uncertainties in the sea surface topography compared to that required for accurate determination of freeboard. Unknown snow depth introduces the largest uncertainty in the conversion of freeboard to ice thickness. Surface roughness is also derived, for the first time, from the variability of successive elevation estimates along the altimeter track. Overall, these ICESat measurements provide an unprecedented view of the Arctic Ocean ice cover at length scales at and above the spatial dimension of the altimeter footprint of ~70 m. *INDEX TERMS:* 1640 Global Change: Remote sensing; 1863 Hydrology: Snow and ice (1827); 4207 Oceanography: General: Arctic and Antarctic oceanography. **Citation:** Kwok, R., H. J. Zwally, and D. Yi (2004), ICESat observations of Arctic sea ice: A first look, *Geophys. Res. Lett.*, *31*, L16401, doi:10.1029/2004GL020309.

1. Introduction

[2] The primary objective of the ICESat mission, launched in 2003, is to measure changes in the elevation of the Greenland and Antarctic ice sheets [*Zwally et al.*, 2002]. ICESat carries a laser altimeter system (GLAS) with two channels, at 1064 nm and 532 nm; the longer wavelength of which is used for surface altimetry. With a beamwidth of ~110 urad and a pulse rate of 40 per second, it samples the Earth's surface from an orbit with inclination of 94° with footprints of ~70 m in diameter spaced at 170-m intervals. Expected accuracy in elevation determination over relatively simple surfaces (e.g., ice sheet) is ~15 cm.

[3] One secondary objective of the mission is to provide estimates of sea ice thickness. Because of the importance of thickness in sea ice mass balance and in the heat and energy budget at the surface, remote determination of ice thickness at almost any spatial scale has long been desired. Current spaceborne sensors, however, can see only radiation emitted or scattered from the top surface or the volume within the top few tens of centimeters of the ice and do not see the lower surface. Thus, an attractive approach has been to use altimetric freeboard with the assumption of hydrostatic equilibrium to determine ice thickness. The first example of ice freeboard measurements from radar altimeters is given by *Laxon et al.* [2003]; specular radar returns from open water/thin ice provide the necessary sea surface reference. Here, we provide a first examination of the ICESat sea ice elevation dataset with a focus on its utility for freeboard determination and thickness estimation over the Arctic Ocean sea ice cover.

0094-8276/04/2004GL020309

2. Data Description

[4] The ICESat sea ice altimetry dataset used here was acquired during a 16-day period between March 4 and March 20, 2003. As seen here, of the ancillary data that are provided with each elevation sample, the altimetric waveform, the reflectivity, and detector gain are the most useful parameters for looking at the ice. Using the gain and received waveform pulse-width, unreliable elevation retrievals due to saturation and atmospheric scattering are removed in the following analysis. We find the coverage (Figure 1) to be quite remarkable because of the large number of valid surface returns and the small number of gaps due to atmospheric contamination and obscuration. We attribute this to effective laser penetration of the cold dry winter atmosphere at this wavelength. To assess the noise level in the elevation retrieval process, we examine the population with the smallest roughness measure in the roughness distributions over the period. Our surface roughness measure is the standard deviation of the ICESat elevations over a 10-km (~60 samples) window after the linear trend in the data has been removed. The lower limit in the observed roughness is in the range ~1.5–2 cm: an indication of the precision in retrieval over smooth surfaces, consistent with the 1.5 cm range precision in a pre-flight test. These smoothest areas are typically found over ice in new leads, the fast first-year ice formed in the passages and straits within the Canadian Archipelago, and the first-year ice just north of Siberia in the E. Siberian and Laptev Seas. Over rougher surfaces, the associated uncertainty could be higher.

3. Results and Discussion

3.1. Freeboard and Thickness Estimation

[5] Figure 2 shows two local freeboard (distance between local sea surface and air-snow interface) and ice draft profiles estimated along two 160 km ICESat tracks: one from an area north of Ellesmere Island (Figure 2a) and the

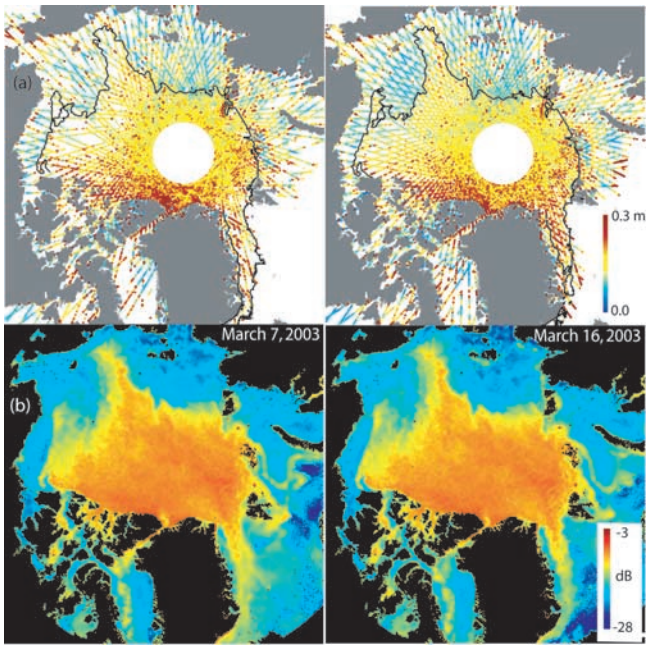

Figure 1. Coverage of the ICESat dataset used here. Surface roughness at a 10-km length scale from ICESat elevations compared with edge of perennial ice zone (PIZ) and backscatter from QuikSCAT. (a) ICESat roughness composites from Day 62–70 and Day 71–79, 2003 with overlaid QuikSCAT PIZ boundary. (b) QuikSCAT backscatter fields on Days 66 and 75.

other from an area in the E. Siberian Sea just north of the Siberian coast (Figure 2f). Geoidal variations and sea surface topography compared to that required for accurate determination of freeboard are not known. Thus, a necessary first step to determine the freeboard from ICESat elevations (shown in Figures 2c and 2h) is to estimate the local sea level by identifying segments along the tracks with known ice thickness i.e., open water or thin ice in leads. The relative flat areas and local minimums along the ICESat profiles (Figures 2c and 2h) are indicative of areas of thinner ice or open water. Further evidence of the case is that these segments are associated with low values in the reflectivity profiles seen in Figures 2d and 2i. Thin ice-filled leads (e.g., grey ice and grey-white ice) have lower reflectivity than snow-covered ice and thick ice. At this writing, the reflectivity is not a calibrated quantity because the GLAS detector saturation and atmospheric attenuation correction algorithms are not finalized. Otherwise, the reflectivity would serve as an ideal indicator of thin ice or open water. The overshoots seen in the reflectivity profiles are artifacts caused by saturation of the GLAS detector amplifier during dark-to-bright transitions. The elevations associated with the reflectivity overshoot are removed in the calculations. Since the flight directions shown here are from left-to-right, the overshoots occur on the right edge of the leads.

[6] Our approach to estimate the thickness of these segments is to examine these leads in time-sequential SAR imagery. RADARSAT imagery at approximately the same spatial resolution (~150 m) allows a closer inspection of the sea ice features along the ICESat track. Additionally, sequential looks at these features allow us to determine the ice age and the approximate ice thickness of these recent openings in the ice cover [*Kwok and Cunningham*, 2002]. Figures 2b and 2g shows two pairs of RADARSAT imagery separated by less than five days. In particular, Figure 2b shows six visible leads that opened between image acquisitions. This provides positive confirmation that these are indeed thin ice leads where the chronological age of the ice is between 0–5 days old. To estimate the thickness of the sea ice in these leads, we use Lebedev's parameterization of sea ice growth rate where $h = 1.33\ F^{0.58}$ (h is thickness and F is the accumulated freezing-degree days derived from NCEP 2-meter air temperature fields). This relationship is based on 24 station years of observations from various locations in the Soviet Arctic and describes ice growth under "average" snow conditions. Under Arctic conditions, growth is fast initially but slows down quickly. Using this growth model and air temperature, we estimate that the range of ice thickness in these leads to be between 0–25 cm with a corresponding range (or uncertainty) of freeboard of ~0–2.5 cm. Errors in freeboard determination associated with uncertainties in the thickness estimates is small since only 11% of the floating ice is above the ocean surface; thus reducing sensitivity. The effect of uncertainty in the ice thickness within the open leads is as follows: thicker/thinner ice estimated covering the leads would give a higher/lower freeboard. For the thickness of the leads in Figure 2b (and similarly in Figure 2g) we use an age that is half the time-separation between the RADARSAT image pairs, giving an uncertainty of <1.5 cm.

[7] The established freeboard thickness at the leads are then used as references to level the ICESat elevation profiles; the resulting freeboard profiles are those shown in Figures 2c and 2h. Obviously, residual tilts due to the short length-scale geoid variations can be reduced if a larger number of thin ice leads are available within the track of interest.

[8] With the resulting freeboard profile, the remaining uncertainty in the conversion of observed freeboard to ice thickness is the depth of the snow cover. Because the laser altimeter returns are from near the top of the air-snow interface and because snow is approximately one-third the density of sea ice, the relative uncertainty in ice thickness as a result of the uncertainty in snow depth is large. As there are no routine snow depth measurements over sea ice, we resort to the snow climatology given by *Warren et al.* [1999]. In March, the climatological snow depths are 32 cm and 12 cm (uncertainty in the fit to the data is ~10 cm) at the two locations shown here. However, these snow depths are constructed from sampling of the snow cover over thick relative level ice. Here, we apply the snow cover via a sigmoidal function (to prevent the snow depth from becoming greater than freeboard) where the snow depth is dependent on ice thickness (see inset, Figure 2h). Admittedly, this avoids the topic of the spatial distribution of snow cover over complex sea ice terrain. But, it serves to illustrate the issues for consideration in the estimation of sea ice thickness at this resolution. With assumed densities of ice (ρ_I = 928 kg/m^3) and snow (ρ_s = 300 kg/m^3), the resulting sea ice thickness profiles from the above steps are shown in Figures 2c and 2h.

[9] The mean ice thickness (3.9 m and 2.7 m) and thickness distributions of the two areas are shown in

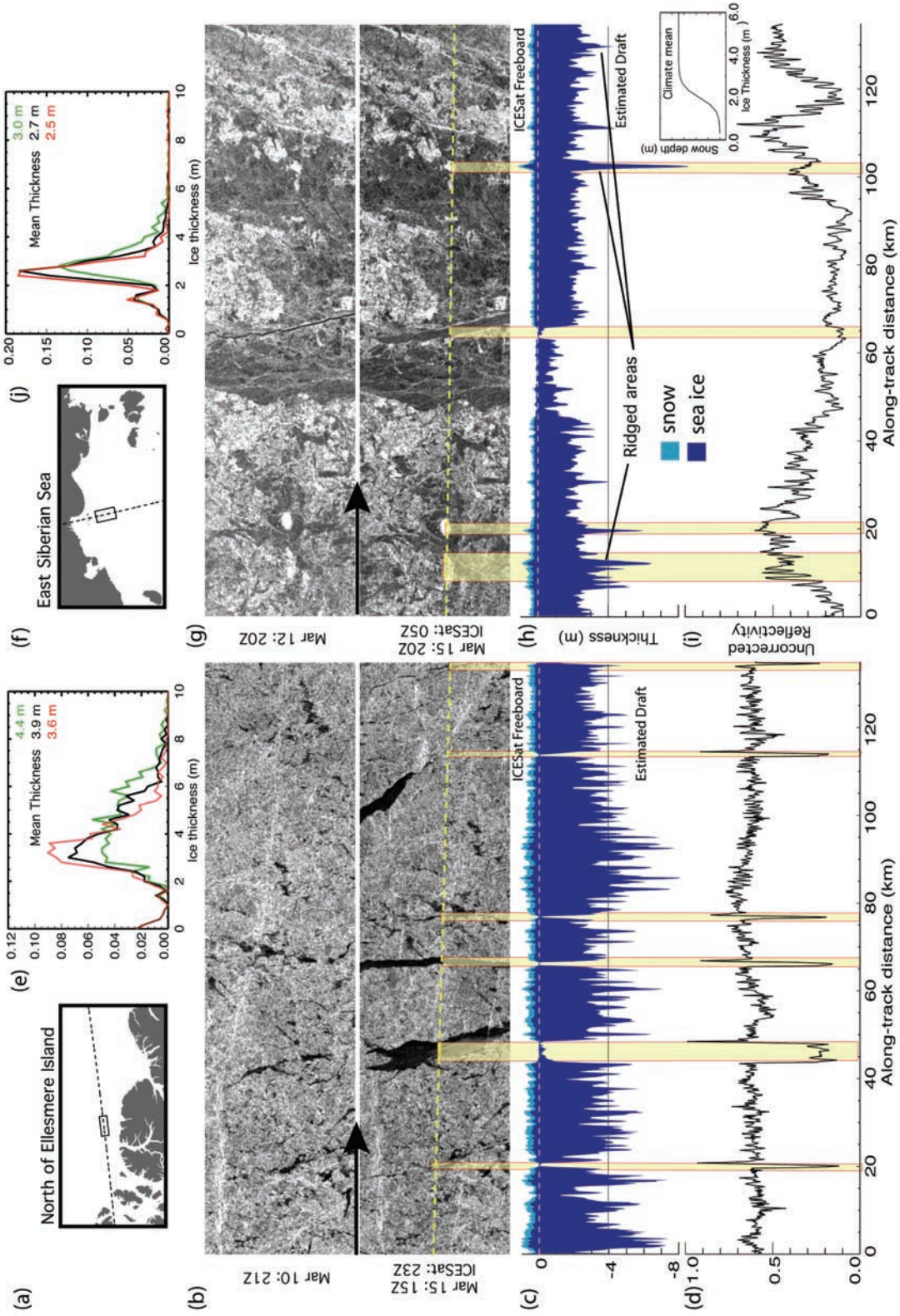

Figure 2. Two near-coincident RADARSAT and ICESat datatakes. (a, f) Geographic location of data. (b, g) ICESat track (dashed yellow line) and new leads/openings seen in time-separated RADARSAT images over the same area on the ice cover. (c, h) ICESat freeboard profile and estimated ice draft (snow: light blue; ice: dark blue). (d, i) Uncorrected reflectivity along the track. (e, j) The thickness distribution with three superimposed snow covers (red: climatological mean+10 cm; black: mean; green: mean−10 cm). (RADARSAT imagery ©CSA 2004). The inset in (i) shows the sigmoidal function for applying snow depth. The vertical scale depends on the climatological snow depth at the geographic location of interest. Yellow bands highlight features referred to in the text.

Figures 2e and 2j. To assess the sensitivity of the mean ice thickness to changes in snow depth, we varied the depth by 10 cm. A ±0.5 m and ±0.25 m change in the mean is seen. Increasing/decreasing the snow depth decreases/increases the mean ice thickness. The effect is more significant over thicker ice as we assumed that the snow cover is deeper over thicker ice.

[10] In addition to providing estimates of the ice age of openings in the ice cover, the RADARSAT imagery provides a spatial context for interpretation of the ICESat elevation profiles. The primary ice type of the area in Figure 2b is generally thicker/rougher multiyear (MY) ice (characterized by high radar backscatter) while that shown in Figure 2g contains a mixture of MY and thinner/smoother first-year (FY) ice (lower backscatter). Correspondingly, the relative reflectivity is stable and higher over MY ice (Figure 2b) but has higher variability over the mixed ice cover (Figure 2g). Again, we note that the reflectivity is not calibrated and is not indicative of their absolute levels at this time. The sensitivity of the profiles to sea ice ridges or contrasts in thickness can be seen at a number of points along the track; visibility is however limited by the resolution of the images in print. The best illustration can perhaps be seen in the four areas in Figure 2g. There are two thick MY floes (∼2–3 km) embedded in FY ice and two ICESat segments that cross what appears to be thicker and more highly-ridged areas that contribute to the population of the tails of the thickness distribution. This combination of RADARSAT and ICESat is potentially useful for understanding ridge statistics at a local scale.

3.2. Surface Roughness

[11] The ability to characterize surface roughness at length scales at and above the spatial dimension of the altimeter footprint of 70 m is a capability unique to resolution ICESat. For the first time, this dataset allows an examination of the surface roughness over the entire Arctic ice cover (defined above, Section 2). Future results on smaller scale roughness should be obtainable from the broadening of laser return waveforms as pulse saturation problems are resolved The spatial distribution of roughness from the two 8-day periods can be seen in Figures 1a and 1b. The approximate range of roughness is from several centimeters (corresponding to the noise level of the retrieval process) to ∼30 cm. As expected, the spatial character of the roughness field remains almost unchanged between the two periods. Variability can be attributed to the advection of different ice areas into the repeat tracks of the altimeter. Overall, the ice cover is roughest north of Ellesmere Island and Greenland (∼30 cm), less rough over much of the central Arctic with MY cover (∼20 cm), and smoothest in the seasonal ice zone (∼10 cm). This spatial character of the roughness field can be compared to the backscatter field from QuikSCAT – a K_u-band scatterometer with spatial resolution of the order of ∼10 km. The scatterometer fields provide delineations of the boundary between the perennial ice zone and seasonal ice zones because of the distinct differences in the backscatter from FY (lower backscatter) and MY (higher backscatter) ice [*Kwok et al.*, 1999]. Even though the radar scattering cross-section is dependent on more than just surface roughness, the correspondence between the changes in surface roughness and backscatter in the transition from the PIZ to the SIZ is quite remarkable.

4. Conclusions

[12] We have provided a first examination of the utility of ICESat derived elevation for determination of sea ice freeboard, the estimation of sea ice thickness, and the characterization of sea ice roughness. The precision of the retrievals (∼2 cm over smooth ice) provides high fidelity profiling of a sea ice cover with expected freeboard variability from centimeters (thin ice) to tens of centimeters (thick MY ice).

[13] Since only 11% of the floating ice is above the ocean surface, freeboard determination errors are magnified when applied to estimating ice thickness and care should be exercised in the definition of the sea level reference. Locally, we demonstrate an approach to obtain these references. Near-coincident RADARSAT and ICESat observations allow us to identify and estimate the ice thickness of open leads for estimation of the sea level. Without surface references, centimetric description of the spatially and temporally varying sea surface topography would be crucial for accurate determination of sea ice freeboard at the basin scale. However, geoidal variations and sea surface topography compared to that required for accurate determination of freeboard are not known. Therefore, approaches to establish the sea-level reference remain a requirement.

[14] Unknown snow depth is the largest source of uncertainty in the conversion to ice thickness. Depending on snow depth and freeboard, this uncertainty could be more than a meter. As the depth of the snow cover is spatially and seasonally variable, a better approach for estimating the snow component of the freeboard needs to be developed.

[15] Examination of the surface roughness field at the Arctic scale shows distinct zones that correspond to regions with primarily perennial ice and seasonal ice. This surface roughness field could be potentially useful for better description of the spatially-varying air/ice and ice/ocean drag coefficients used in calculating air/ice/ocean momentum exchanges.

[16] This ICESat dataset represents a significant advancement in the observation of Arctic Ocean sea ice cover and sea ice freeboard. These high-resolution ICESat measurements are useful for estimation of sea ice thickness and surface roughness at length scales at and above the spatial dimension of the altimeter footprint. Due to the shorter than expected operating lifetime of ICESat's three lasers, periods of data collection are limited to about 33 days each for perhaps a total of 8 periods over 3 years instead of the planned continuous operation for 3 to 5 years. The impact of such data for climate and sea ice studies would be enormous if continual long-term direct observations of ice freeboard and thence ice thickness could be realized.

[17] **Acknowledgments.** The March 12–20 data were obtained from the National Snow and Ice Data Center (www.nsidc.org), and data for March 4–12 are preliminary cal/val period data. We wish to thank Glenn Cunningham for his software support at JPL. RK performed this work at the Jet Propulsion Laboratory, California Institute of Technology under contract with the National Aeronautics and Space Administration, and the work of JZ and DY is supported by NASA's funding of the ICESat/GLAS Science Team.

References

Kwok, R., and G. F. Cunningham (2002), Seasonal ice area and volume production of the Arctic Ocean: November 1996 through April 1997, *J. Geophys. Res.*, *107*(C10), 8038, doi:10.1029/2000JC000469.

Kwok, R., G. F. Cunningham, and S. Yueh (1999), Area balance of the Arctic Ocean perennial ice zone: October 1996 to April 1997, *J. Geophys. Res.*, *104*, 25,747–25,749.

Laxon, S., N. Peacock, and D. Smith (2003), High interannual variability of sea ice in the Arctic region, *Nature*, *425*, 947–950.

Warren, S. G., I. G. Rigor, N. Untersteiner, V. F. Radionov, N. N. Bryazgin, Y. I. Aleksandrov, and R. Colony (1999), Snow depth on Arctic sea ice, *J. Clim.*, *12*, 1814–1829.

Zwally, H. J., et al. (2002), ICESat's laser measurements of polar ice, atmosphere, ocean, and land, *J. Geodyn.*, *24*, 405–445.

R. Kwok, Jet Propulsion Laboratory, California Institute of Technology, 4800 Oak Grove Drive, Pasadena, CA 91109, USA. (ron.kwok@jpl.nasa.gov)

D. Yi and H. J. Zwally, Goddard Space Flight Center, Code 971, Greenbelt, MD 20771, USA.